# *Notes*

## Synthesis and Structural Studies on $[Mg_3(O_2CC{\equiv}CSiMe_3)_6(HMPA)_4]$: Mechanistic Implications for the Formation of the $\mu_4$-$\eta^4$ Bonding Type in Carbamato-Bridged $Mg_6$ Cage Compounds

Kuo-Ching Yang,[†,§] Chung-Cheng Chang,*[,‡] Charng-Sheng Yeh,[§] Gene-Hsiang Lee,[⊥] and Yu Wang[⊥]

*Department of Chemical Engineering, Chengshiu Institute of Technology, Kaohsiung, Taiwan, Republic of China, Department of Applied Chemistry, National University of Kaohsiung, Kaohsiung, Taiwan, Republic of China, Department of Chemistry, National Sun Yat-Sen University, Kaohsiung, Taiwan, Republic of China, and Department of Chemistry, National Taiwan University, Taipei, Taiwan, Republic of China*

*Received July 10, 2001*



*Summary: The insertion reaction of $CO_2$ with $Mg(C{\equiv}CSiMe_3)_2$ was characterized by NMR spectroscopic studies to give a cage compound $[Mg_n(O_2CC{\equiv}CSiMe_3)_{2n}\cdot(THF)_m]$, **1a**, and the addition of HMPA/THF (HMPA = hexamethylphosphoramide) to solutions of **1a** produces a trimeric compound, $[Mg_3(O_2CC{\equiv}CSiMe_3)_6(HMPA)_4]$, **1b**. X-ray diffraction studies of this showed **1b** to contain a completely centrosymmetric linear array of magnesium atoms linked with $\mu_2$-$\eta^2$- and $\mu_2$-$\eta^3$-$O_2CC{\equiv}CSiMe_3$. It was found to be a key compound in the mechanism leading to the formation of $\mu_4$-$\eta^4$ bonding in carbamato-bridged $Mg_6$ cage compounds.*

### Introduction

Carbon dioxide has a Lewis basic oxygen atom, which binds to a metal center, generally leading to the activation of the carbon dioxide molecule, and several bonding modes have been described.[1] Studies on metal−carbon dioxide compounds may provide both structural and functional models for surface-bound intermediates in catalytic conversion processes.[2] Previously, we have reported that the insertion of carbon dioxide into the Mg−C and Mg−N bonds of magnesium compounds yields linear trimeric and cage compounds, both involving various bonding modes between the carboxylato or carbamato ligands and the magnesium atom, including types **c** ($\mu_2$-$\eta^2$), **d** ($\mu_2$-$\eta^3$), **e** ($\mu_3$-$\eta^3$), and **g** ($\mu_4$-$\eta^4$), as shown in Figure 1.[3] Crystallographic studies have shown than steric repulsion of ligands causes bending linear trimers, to give a cage compound. Because the tetradendate $\mu_4$-$\eta^4$-carbamato ligand can only be observed in a cage compound,[3] it is important to understand the detailed bonding modes. In this study, after we obtained the structural data for the new compound $[Mg_3(O_2CC{\equiv}CSiMe_3)_6(HMPA)_4]$, **1b** (HMPA = hexamethylphosphoramide), we then could make comparisons between it and the known $[Mg_3(O_2C^iPr)_6(HMPA)_2]$, **2**, and $[Mg_3(O_2CNMe_2)_6(HMPA)_2]$, **3**.[3] By comparing these compounds, we could understand which bonding path is involved in the recombination of type **c** ($\mu_2$-$\eta^2$) into type **g** ($\mu_4$-$\eta^4$).

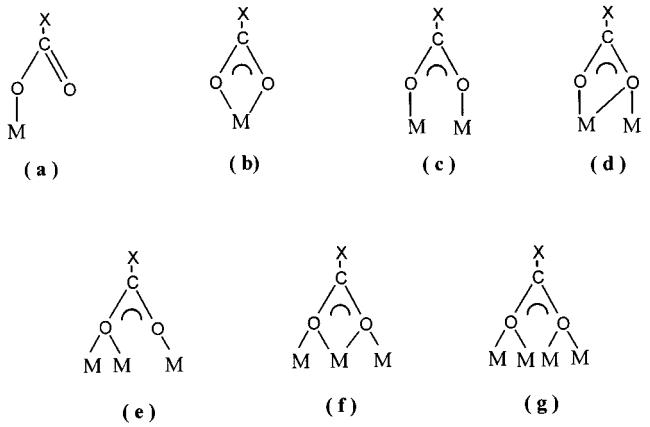


**Figure 1.** Possible bonding types of carboxylato (X = C) and carbamato (X = N) ligands: (**a**) $\eta^1$; (**b**) $\eta^2$; (**c**) $\mu_2$-$\eta^2$; (**d**) $\mu_2$-$\eta^3$; (**e**) $\mu_3$-$\eta^3$; (**f**) $\mu_3$-$\eta^4$; (**g**) $\mu_4$-$\eta^4$.

### Results and Discussion

On bubbling an excess of gaseous $CO_2$ into an $Mg(C{\equiv}SiMe_3)_2$ solution in THF for 20 min, an intermediate exothermic reaction occurred. After adding hexane to

[†] Chengshiu Institute of Technology.
[‡] National University of Kaohsiung.
[§] National Sun Yat-Sen University.
[⊥] National Taiwan University.

(1) (a) Leitner, W. *Coord. Chem. Rev.* **1996**, *153*, 257. (b) Costamagna, J.; Ferraudi, G.; Canales, J.; Vargas, J. *Coord. Chem. Rev.* **1996**, *148*, 221. (c) Darensbourg, D. J.; Holtcamp, M. W. *Coord. Chem. Rev.* **1996**, *153*, 155. (d) Leitner, W. *Angew. Chem., Int. Ed. Engl.* **1995**, *34*, 2207. (e) Jessop, P. G.; Ikariya, T.; Noyori, R. *Chem. Rev.* **1995**, *95*, 259. (f) Behr, A. *Angew. Chem., Int. Ed. Engl.* **1988**, *27*, 661. (g) Braunstein, P.; Matt, D.; Nobel, D. *Chem. Rev.* **1988**, *88*, 747. (h) Palmer, D. A.; van Eldik, R. *Chem. Rev.* **1983**, *83*, 651. (i) Ruben, M.; Walther, D.; Knake, R.; Görls, H.; Beckert, R. *Eur. J. Inorg. Chem.* **2000**, 1055.
(2) Gibson, D. H. *Coord. Chem. Rev.* **1999**, *185*, 335.
(3) Yang, K.-C.; Chang, C.-C.; Yeh, C.-S.; Lee, G.-H.; Peng, S.-M *Organometallics* **2001**, *20*, 126.

10.1021/om010615k CCC: $22.00 
Publication on Web 02/16/2002

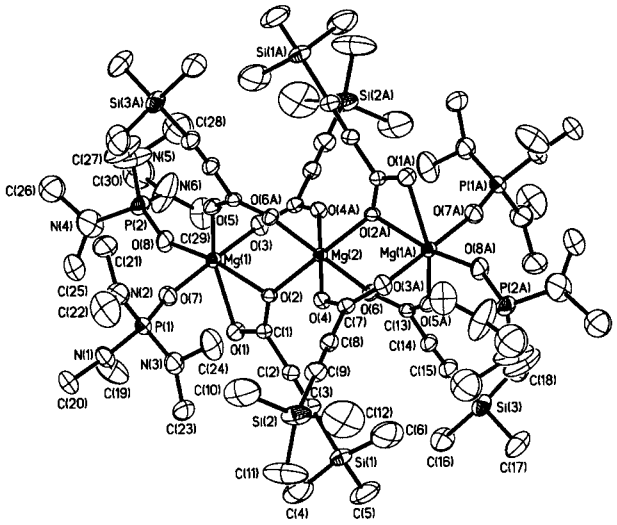


**Figure 2.** ORTEP view of the molecule **1b** using 30% probability ellipsoids. Important bond lengths (Å) and bond angles (deg): Mg(1)−O(8) 1.998(2), Mg(1)−O(7) 2.013(3), Mg(1)−O(5) 2.028(2), Mg(1)−O(3) 2.063(2), Mg(1)−O(2) 2.138(2), Mg(1)−O(1) 2.291(2), Mg(1)···Mg(2) 3.6013(9), Mg(2)−O(6) 2.068(2), Mg(2)−O(4) 2.072(2), Mg(2)−O(2) 2.072(2), O(1)−C(1) 1.244(4), O(2)−C(1) 1.274(3), O(3)−C(7A) 1.252(4), O(4)−C(7) 1.242(2), O(5)−C(13A) 1.257(4), O(6)−C(13) 1.242(4), O(8)−Mg(1)−O(7) 91.0(1), O(8)−Mg(1)−O(5) 101.7(1), O(7)−Mg(1)−O(5) 91.0(1), O(8)−Mg(1)−O(7) 88.2(1), O(7)−Mg(1)−O(3) 177.8(1), O(5)−Mg(1)−O(3) 91.2(1), O(8)−Mg(1)−O(2) 163.0(1), O(7)−Mg(1)−O(2) 91.5(1), O(5)−Mg(1)−O(2) 95.12(9), O(3)−Mg(1)−O(2) 88.71(9), O(8)−Mg(1)−O(1) 104.2(1), O(7)−Mg(1)−O(1) 84.7(1), O(5)−Mg(1)−O(1) 153.9(1), O(3)−Mg(1)−O(1) 93.5(1), O(2)−Mg(1)−O(1) 59.32(8), O(8)−Mg(1)−O(7), O(6)−Mg(2)−O(6A) 180.0, O(6)−Mg(2)−O(4) 91.76(9), O(6)−Mg(2)−O(4A) 88.24(9), O(4)−Mg(2)−O(4A) 180.0, O(6)−Mg(2)−O(2) 90.66(8), O(4)−Mg(2)−O(2) 89.60(8) O(6)−Mg(2)−O(2A) 89.34(8), O(4)−Mg(2)−O(2A) 90.40(8), O(2)−Mg(2)−O(2A) 180.0.

the resulting solution and storing it at 0 °C, a cage compound $[Mg_n(O_2CC{\equiv}CSiMe_3)_{2n}{\cdot}(THF)_m]$ (**1a**) was produced. Then, by recrystallizing from HMPA/THF (2:1), we obtained colorless crystals of **1b**.

Single-crystal X-ray analysis was carried out on compound **1b** (Figure 2). This new structure consists of discrete trinuclear molecules with a centrosymmetric linear array of magnesium atoms linked by two sets of three $O_2CC{\equiv}CSiMe_3$ ligands, via type **c** and type **d** bonding. About the central magnesium Mg(2) atom there is an almost regular octahedral configuration of the bridging oxygen atoms of the $O_2CC{\equiv}CSiMe_3$ ligands. The outer magnesium atoms Mg(1) and Mg(1A) are additionally coordinated to two HMPA molecules, forming a distorted octahedron. When comparing the linear trinuclear compounds **1b**, **2**, and **3**, several interesting structural differences could be recognized. One difference was that the terminal magnesium atoms in **2** and **3** are pentacoordinate with one additional HMPA molecule. Another difference was that the Mg···Mg distance of 3.601(1) Å in **1b** is longer than that of 3.496(1) Å in **2** and 3.459(1) Å in **3**. Still another difference is that larger OCO angles were observed in **1b** (Table 1). Finally, another important difference is that the distances $Mg_t-O_b$ and $Mg_t-O_t$ in the four-membered ring, $Mg_tO_tCO_b$, are different. In **1b**, the distance between terminal magnesium and the bridging oxygen, Mg(1)−O(2), 2.138(2) Å, is shorter than the distance Mg(1)−O(1), 2.291(2) Å, making the $Mg_t-O_b$ stronger. In striking contrast, **2** and **3** exhibit a weak interaction between the terminal magnesium and the bridging oxygen atoms (Table 1). Therefore, we divided type **d** into two modes: type **d-1** and **d-2** (Table 1). Additionally, the C(1)−O(1) bond length of 1.244(4) Å in **1b** exhibits a stronger double-bond character than does the other C(1)−O(2) bond [1.274(3) Å].[4] This is shown also by the IR absorption band at 1645 $cm^{-1}$.[5,6] In fact, Parkin has reported finding an $\eta^1$-coordination mode of the acetato ligand in his magnesium compound $\{\mu_3$-HB(3-$^t$BuPz)$_3\}$Mg($\eta^1$-$O_2CCH_3$), **4**, which also has a C═O bond.[7] A **d-2** mode after the cleavage of $Mg_t$ and $O_t$ becomes the **d-3** mode, which involves $\eta^1$-coordination similar to that in **4**.

In summary at this point, we propose the reaction path shown in Scheme 1, which could be supported in part by the variable-temperature NMR spectra discussed in the next section. First, a trimer with type **c** bonding forms an intramolecular dative bond between the bridging oxygen atom $O_b$ and the terminal magnesium atom $Mg_t$, producing a type **d-1** bond.[8] Second, the stronger bond $Mg_t-O_b$ forms and generates the type **d-2**

**Table 1. Bond Lengths (Å) and Bond Angles (deg) for the Compounds 1b, 2, and 3**

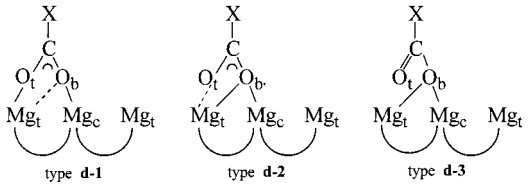


$Mg_t$ : terminal magnesium, $Mg_c$ : central magnesium, * : the O-C-O angle of type **b**

--- : weak bond, — : strong bond.

| | 1b | 2 | 3 |
|---|---|---|---|
| $Mg_t-Mg_c$ | 3.601(1) ($Mg_1-Mg_2$) | 3.496(1) ($Mg_1-Mg_2$) | 3.459(1) ($Mg_1-Mg_2$) |
| $O_t-C-O_b$ | 121.4(3) ($O_1-C_1-O_2$) | 118.5(2) ($O_5-C_9-O_6$) | 119.2(2) ($O_2-C_7-O_3$) |
| O−C−O* | 128.8(3) ($O_{3A}-C_7-O_4$) | 125.9(3) ($O_1-C_1-O_2$) | 125.8(2) ($O_4-C_{10}-O_5$) |
| O−C−O* | 127.9(3) ($O_{5A}-C_{13}-O_6$) | 124.3(3) ($O_3-C_5-O_4$) | 123.5(2) ($O_6-C_{13}-O_7$) |
| $Mg_c-O_b$ | 2.072(2) ($Mg_2-O_2$) | 2.075(2) ($Mg_1-O_5$) | 2.094(2) ($Mg_1-O_2$) |
| $Mg_t-O_b$ | 2.138(2) ($Mg_1-O_2$) | 2.181(2) ($Mg_2-O_5$) | 2.179(2) ($Mg_2-O_2$) |
| $Mg_t-O_t$ | 2.291(2) ($Mg_1-O_1$) | 2.091(2) ($Mg_2-O_6$) | 2.079(2) ($Mg_2-O_3$) |
| $C-O_b$ | 1.274(3) ($C_1-O_2$) | 1.266(3) ($C_9-O_5$) | 1.271(3) ($C_7-O_2$) |
| $C-O_t$ | 1.244(4) ($C_1-O_1$) | 1.257(3) ($C_9-O_6$) | 1.267(3) ($C_7-O_3$) |

**Scheme 1**

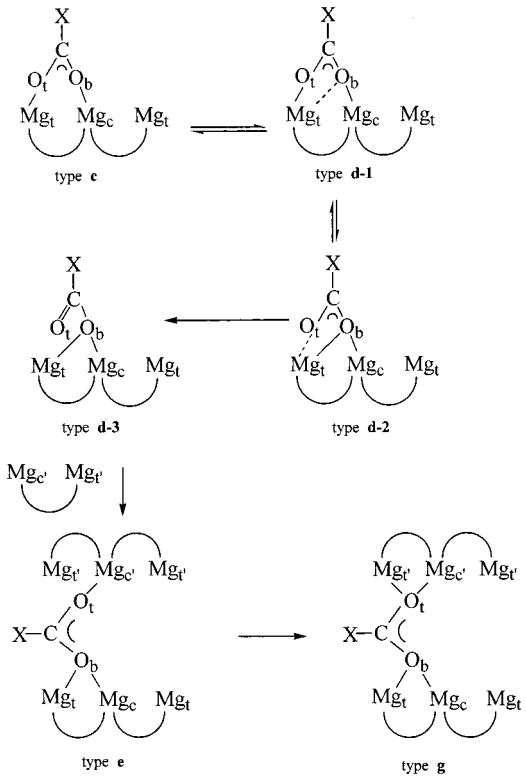


mode. Third, $Mg_t-O_t$ bond cleavage results in an intermediate type **d-3** mode. Finally, the other trimer attacks, forming types **e** and **g**. If **d-2** is formed first, followed by **d-1**, no bond cleavage could occur to generate free oxygen $O_t$, and, thus, there would be no recombination with the other trimer.

In an $^1$H NMR spectroscopic study of **1a** (in benzene-$d_6$), the methyl proton resonance of the C≡CSiMe$_3$ group appeared as a complicated overlapping multiplet in the region of 0.18−0.69 ppm, and the $^{13}$C NMR spectrum of the methyl carbon atoms of the C≡CSiMe$_3$ group appeared as many distinct signals in the region 0.10−1.86 ppm. Such spectral complexity is similar to that observed in one of our previous cage compounds, [$Mg_6(O_2CNEt_2)_{12}$][3] (Figure 3), which can be considered as favored by a recombination step to get the final product. The $^{13}$C NMR spectrum of **1a** showed a signal at 160.26 ppm, assignable to the quaternary carbon atoms of the $CO_2$ groups.[9] In the $^1$H NMR spectrum (benzene-$d_6$) of **1b**, the singlet at $\delta$ 0.16 ppm and the doublet at 2.54 ppm were assigned to the methyl protons of the trimethylsilyl group and HMPA, respectively. In the $^{13}$C NMR spectrum, the quaternary carbon atom of the $CO_2$ group appeared at $\delta$ 159.69 ppm.[9] A $^1$H NMR and $^{31}$P NMR variable-temperature study was carried out on **1b** between −60 and 50 °C in THF-$d_8$ solution. At 30 °C,

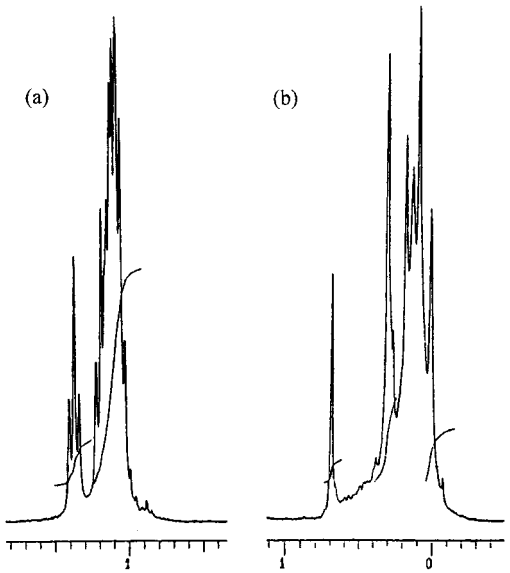


**Figure 3.** $^1$H NMR spectra (benzene-$d_6$) of [$Mg_6(O_2CNEt_2)_{12}$] (a) and **1a** (b) in the $CH_3$ region.

the $^1$H NMR spectrum showed one singlet at 0.15 ppm and one doublet at 2.65 ppm for the methyl protons of the trimethylsilyl group and HMPA, respectively. At −60 °C, two sets of singlets were observed at 0.13 and 0.14 ppm and two sets of doublets at 2.56 and 2.68 ppm. Because two bulky and stronger HMPA donor bases on the terminal magnesium atoms stabilized **1b** and prevented recombination in THF-$d_8$ solution, we did not observe the complicated overlapping appearance due to cage formation in the methyl region. Similarly, at 50 and 30 °C, the $^{31}$P NMR spectrum of **1b** showed one signal at 24.51 and 24.38 ppm, corresponding to the phosphorus atom of HMPA. At −60 °C, the HMPA signal split into two distinct signals, one at 23.53 and the other at 24.00 ppm. These signals arose from two different phosphorus species, which was consistent with the solid structures, which have two types of HMPA donor ligands.

## Experimental Section

**General Data.** All experiments were carried out in an $N_2$-flushed glovebag, in a drybox, or in a vacuum line using standard Schlenk techniques. Magnesium metal and trimethylsilylacetylene were purchased from Aldrich and used as received. Mg(C≡CSiMe$_3$)$_2$ was prepared by following previous reports.[10] All solvents were distilled and degassed prior to use. All $^1$H, $^{13}$C, and $^{31}$P spectra were measured on a Varian-200, 300, or 500 spectrometer. Chemical shifts are referenced to either TMS or deuterated solvent as an internal standard. $^{31}$P NMR spectra were referenced to external 85% $H_3PO_4$. IR spectral data were obtained on an FT-IR spectrometer. Elemental analyses (C, H, and N) were performed by the Analytsche Laboratorien of H. Malissa and G. Reuter, GmbH, Germany.

The crystal was mounted on a glass fiber using expoxy resin, transferred to a goniostat, and cooled to 220 K under liquid nitrogen vapor. Data were collected on a Bruker SMART CCD diffractometer using graphite-monochromatized Mo Kα radiation ($\lambda$ = 0.71073 Å). Structural determinations were made using the SHELXTL program package. All refinements were carried out by full-matrix least squares using anisotropic

(4) (a) Huheey, J. E. *Inorganic Chemistry*; Harper & Row Publishers: New York, 1974. (b) Ye, B. H.; Mak, T.; Williams, I. D.; Li, X. Y. *J. Chem. Soc., Dalton Trans.* **1998**, 1935.
(5) (a) Aresta, M.; Dibenedetto, A.; Quaranta, E. *J. Chem. Soc., Dalton Trans.* **1995**, 3359. (b) Arduini, A. L.; Jamerson, J. D.; Takats, J. *Inorg. Chem.* **1981**, *20*, 2474. (c) Deacon, G. B.; Phillips, R. J. *Coord. Chem. Rev.* **1980**, *33*, 227. (d) Calderazzo, F.; Dell'Amico, G.; Netti, R.; Pasquali, M. *Inorg. Chem.* **1978**, *17*, 471.
(6) Randhawa, H. S. *Vib. Spectrosc.* **1994**, *7*, 79.
(7) Han, R.; Parkin, G. *J. Am. Chem. Soc.* **1992**, *114*, 748.
(8) Caudle, M. T.; Kampf, J. W. *Inorg. Chem.* **1999**, *38*, 5474.
(9) Gibson, D. H. *Chem. Rev.* **1996**, *96*, 2063.
(10) (a)Schubert, B.; Behrens, U.; Weiss, E. *Chem. Ber.* **1981**, *114*, 260. (b) Geissler, M.; Kopf, J. *Chem. Ber.* **1981**, *122*, 1395.

**Table 2. Crystal and Intensity Collection Data for Compound 1b**

| | |
|---|---|
| formula | $C_{60}H_{126}Mg_3N_{12}O_{16}P_4Si_6$ |
| fw | 1637.08 |
| cryst syst | triclinic |
| space group | $P\bar{1}$ |
| *a*, Å | 12.2761(2) |
| *b*, Å | 13.9829(1) |
| *c*, Å | 16.4374(1) |
| α, deg | 111.313(1) |
| *β*, deg | 104.555(1) |
| *γ*, deg | 102.939(1) |
| *V*, Å$^3$ | 2383.67(4) |
| *Z* | 1 |
| $D_{calc}$, g/cm$^3$ | 1.140 |
| $\mu$, mm$^{-1}$ | 0.232 |
| *F*(000) | 878 |
| cryst size | 0.42 × 0.40 × 0.40 |
| *θ* range, deg | 1.43 to 26.37 |
| no. of reflns collected | 26 665 |
| no. of indpdt reflns | 9509 ($R_{int}$ =0.0257) |
| transm factor (max, min) | 0.9280, 0.8433 |
| *T*, K | 220(1) |
| GOF | 1.081 |
| final *R* indices [$I > 2\sigma(I)$] | R1 = 0.0696, wR2 = 0.1878 |
| *R* indices (all data) | R1 = 0.0887, wR2 = 0.2026 |
| extinction coeff | 0.0098(15) |
| largest diff peak and hole, e Å$^{-3}$ | 1.070 and −0.553 |

displacement parameters for all non-hydrogen atoms. All hydrogen atoms were calculated. In compound **1b**, one methyl group of each HMPA ligand is disordered. The carbon atoms of C(26), C(28), C(30) and C(26′), C(28′), C(30′) have a 63%/37% occupancy ratio. The crystal data are summarized in Table 2.

**Reaction of Carbon Dioxide with Mg(C≡CSiMe$_3$)$_2$.** An excess of carbon dioxide was bubbled into a solution of Mg(C≡CSiMe$_3$)$_2$ (37.8 mmol) in THF (100 mL) for 20 min, causing an exothermic reaction. After centrifugation, hexane (10 mL) was added, and a microcrystalline solid **1a** was obtained on cooling at 0 °C. Subsequently, the solid was washed with hexane and dried in a vacuum. Then, a 2:1 mixture of HMPA and THF (15 mL) was added to **1a**. The resolution was kept room temperature as the solvent slowly evaporated. Large block crystals of **1b** formed.

**[Mg$_n$(O$_2$CC≡CSiMe$_3$)$_{2n}$·(THF)$_m$], 1a**: $^1$H NMR (benzene-$d_6$) $\delta$ 0.02− 0.30, 0.69 [m, *Me*$_3$Si], 1.53 (br, 3, 4 −thf−*H*), 3.96 (br, 2, 5 −thf−*H*); $^{13}$C NMR (benzene-$d_6$) $\delta$ 0.10, 0.30, 0.36, 0.59, 0.64, 0.84, 1.86 (*Me*$_3$Si), 26.00 (3, 4 −thf −*C*), 69.24 (2, 5 −thf−*C*), 160.26 (*C*O$_2$); IR (KBr, cm$^{-1}$) 1605 s (asm −CO$_2$).

**[Mg$_3$(O$_2$CC≡CSiMe$_3$)$_6$(HMPA)$_4$], 1b**: yield 78%, mp$_{dec}$ > 168 °C; $^1$H NMR (benzene-$d_6$) $\delta$ 0.16 [s, 54H, *Me*$_3$Si], 2.54 [d, 72H, (*Me*$_2$N)$_3$PO]; $^1$H NMR (THF-$d_8$) 0.15 [s, 54H, *Me*$_3$Si], 2.65 [d, 72H, (*Me*$_2$N)$_3$PO]; $^{13}$C NMR (benzene-$d_6$) $\delta$ 0.15, 0.17 (*Me*$_3$-Si), 37.24, 37.28 [(*Me*$_2$N)$_3$PO], 83.90 (Me$_3$SiC≡C), 104.31 (Me$_3$-SiC≡C), 159.89 (*C*O$_2$); $^{13}$C NMR (THF-$d_8$) $\delta$ 0.04 (*Me*$_3$Si), 37.35, 37.39 [(*Me*$_2$N)$_3$PO], 82.91 (Me$_3$SiC≡C), 104.20 (Me$_3$SiC≡C), 159.69 (*C*O$_2$); $^{31}$P NMR (THF-$d_8$) $\delta$ 24.38 [(Me$_2$N)$_3$*P*O]; IR (KBr, cm$^{-1}$) 1599 s (asm −CO$_2$). Anal. Calcd for **1b** ($C_{60}H_{126}$-$Mg_3N_{12}O_{16}P_4Si_6$): C, 44.04; H, 7.71; N, 10.28. Found: C, 44.23; H, 7.67; N, 10.60.

**Acknowledgment.** We thank the National Science Council, Taiwan, ROC, for financial support.

**Supporting Information Available:** Table of crystal data, atomic coordinates and temperature factors, and intramolecular bond distances and angles of **1b** and the complete spectroscopic and analytical data for **1a** and **1b**. This material is available free of charge via the Internet at http://pubs.acs.org.

OM010615K